Journal of Molecular Structure 1312 (2024) 138614

Contents lists available at ScienceDirect

Journal of Molecular Structure

journal homepage: www.elsevier.com/locate/molstr

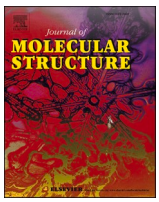

Fingolimod phosphoramidate prodrugs: Synthesis, photophysical characterisation and lipid bilayer interaction of fluorescent tagged Prodrug

Fabrizio Pertusati [a,*], Michaela Serpi [a], Chiara Morozzi [c], Edward James [c], Giacomo Renno [b], Francesca Cardano [b], Andrea Fin [b]

[a] School of Chemistry Cardiff University, Main Building, Park Place, Cardiff, CF10 3AT, United Kingdom
[b] Department of Chemistry University of Turin, Via Pietro Giuria 7, 10125, Torino, Italy
[c] School of Pharmacy and Pharmaceutical Sciences, Redwood Building, King Edward VII Avenue, Cardiff, CF10 3NB, United Kingdom

ARTICLE INFO

Keywords:
Fingolimod phosphate
Prodrug
Fluorescence
Liposomes
Lysosomal storage diseases

ABSTRACT

FTY720 (Fingolimod, Gilenya, **1**), a structural analog of sphingosine (**2**) was the first orally administered drug approved for the treatment of multiple sclerosis (MS). However, the phosphate derivative of Fingolimod, namely Fingolimod-1-phosphate (FTY720-1P, **3**) is the biologically active molecule in MS as well as in various lysosomal storage diseases such as mucolipidosis IV and Nieman-Pick. In all cases, Fingolimod requires to be phosphorylated, resembling the natural sphingosine phosphate (**4**), to accomplish its therapeutic/biological effects. Here, we report the synthesis of a small library of prodrugs that could provide the efficient delivery of **3**, the bioactive species. Moreover, to gain insight about the biological behaviour of these novel candidates within human body such as cell and brain blood barrier penetration we have prepared and spectroscopically characterised a fluorescent tagged version of one of the new prodrugs. The behavior of our prodrugs with respect to biological membranes was evaluated by studying the interaction between the fluorescent prodrug **18** and DOPC/DPPC liposome models.

1. Introduction

FTY720 (Fingolimod, Gilenya, **1**), a fungal metabolite derived from the Chinese herb *Iscaria sinclarii*. (Fig. 1), is a drug approved in 2018 as the first oral treatment for relapsing multiple sclerosis, due to its immunomodulating properties [1].

To exert its biological activity FTY720, in analogy to sphingosine (**2**) needs to be phosphorylated by nuclear sphingosine kinases (SphKs), at one of the two alcohol groups to generate the active metabolite Fingolimod phosphate (FTY720-1P, **3**), which structurally resembles naturally occurring sphingosine 1-phosphate (S1P, **4**) and acts on S1P receptors [2]. Among the two enzymes responsible for the phosphorylation process, sphingosine kinase-2 (*SPHK2*) is capable to phosphorylate FTY-720 30-fold more efficiently than SPHK-1 due to the lower K_M of FTY720 for *SPHK2* [2,3]. Both the prominent S1P expression in neural cells and its widespread effects on the proliferation, differentiation together with the fact that FTY720 is capable of crossing the blood-brain barrier (BBB) make this drug an attractive treatment for diseases with neural pathologies such as lysosomal storage disorders. Indeed, Grishchuk group has shown that FTY720-1P is highly effective at restoring intracellular signalling, reduce cytokine secretion, down-regulate signalling within the PI3K/Akt and MAPK pathways, and restore the lysosomal compartment in Mcoln1$^{-/-}$ astrocytes, a cellular model for Mucolipidosis IV (MLIV), an orphan neurodevelopmental disease caused by loss of function of the lysosomal channel mucolipin-1 [4]. FTY720-1P, acting as histone deacetylase (HDAC) inhibitor [5], was shown to be capable to reduce the cholesterol storage phenotype in fibroblasts derived from patients with Niemann-Pick Type C (NPC) disease, a rare and progressive lysosomal disorder [6]. From these results clearly emerges how the phosphorylation of Fingolimod is essential for the therapeutic effect of the molecule. The direct delivery of FTY720-1P would be highly desirable from the development of new therapeutics point of view. However, the insertion of a phosphate moiety into the Fingolimod scaffold confers a strong polar and hydrophilic character to the prodrug which, of course, improves its solubility in physiological media and prompts the spontaneous aggregation into supramolecular macro-assembly like micelles [7]. Nevertheless, the aggregation into supramolecular constructs, along with the limited ability to cross hydrophobic media such as cell bilayer

* Corresponding author.
E-mail address: pertusatif1@cardiff.ac.uk (F. Pertusati).

https://doi.org/10.1016/j.molstruc.2024.138614
Received 13 January 2024; Received in revised form 16 April 2024; Accepted 11 May 2024
Available online 12 May 2024

membranes and blood-brain barrier, due to the charged anchoring phosphate moiety, narrows or hampers the therapeutic employment and delivery of the drug. Over the years many approaches have been investigated to facilitate the interaction and transport through cell barriers based on small molecules, supramolecular assemblies, macrocyclic, biocompatible polymers and functional small modification [8]. To the latter family belongs the phosphoramidate prodrug strategy which has been successfully applied to substrates that required phosphorylation to achieve biological activity like in the case of many antiviral and anticancer nucleosides and carbohydrates that have led to several marketed drugs [9]. Phosphoramidate technology has been successfully reported by our group on nucleoside-based drugs and, as a proof of concept, on benzyl ether derivatives of S1P1 agonists, demonstrating that the prodrugs monophosphates could be release upon activation by esterase enzymes *in vitro* [10].

In strict analogy with our success in nucleoside-based drugs[9b] we become interested in applying our phosphoramidate technology to Fingolimod to evaluate our prodrugs for their ability to release the active metabolite **3**. As the overall mechanism of action of Fingolimod phosphate in MLIV and NPC is not yet well understood, we expect that a fluorescent tagged version of a molecule that can deliver FTY-1P will be a powerful *molecular* tool for elucidating the underlying mechanism of this molecule in living system. This is of particular interest as it will help to develop potential treatments for rare lysosomal storage diseases, which represent a huge unmet medical need.

In this article, we are reporting the successful synthesis of a small family of FTY720 phosphoramidate prodrugs and demonstrate the activation of compound **9e** and **9d** in neuronal cell lysate. We are also describing the synthesis of a fluorescent tagged derivative, together with its photophysical characterisation and its interaction with liposomes as model for cellular membrane.

2. Results and discussion

2.1. Chemistry

2.1.1. Synthesis of Fingolimod prodrugs

For the synthesis of Fingolimod prodrugs, we applied the well-established phosphorochloridate/Grignard methodology [10,11]. Despite the great success of l-alanine promoiety in commercial phosphoramidates (Sovaldi, Tenofovir alafenamide and ultimately Remdesevir) we were interested in expanding our investigation to other natural amino acids that were never explored before in these prodrugs. For this purpose, we had to prepare the corresponding phosphoramidating agents (**8a-e**), bearing l-methionine ethyl ester, l-tryptophan methyl ester, l-lysine methyl ester, l-dimethoxy-l-glutamic acid, and l-alanine (Scheme 1). Those candidates were indeed selected as unconventional promoieties keeping one example of alanine for comparison. We also explored the nature of the aryloxy moiety with one example each of phenol, 1-naphthyl and 5,6,7,8-tetrahydro-1-naphthyl, a moiety that was found to be quite advantageous for the activity of antiviral nucleosides [12].

With the phosphoramidating agents **8a-e** in hands we attempted the Fingolimod mono phosphorylation at the alcohol moiety. A THF solution of Fingolimod hydrochloride was treated with 1.1 equivalents of *t*BuMgCl (1 M in THF) and the resulting suspension stirred at room temperature for one hour to allow the complete formation of the magnesium salt. Upon the salt intermediate formation, the proper phosphorochloridate (**8a-e**) dissolved in THF were added dropwise over 15–20 min. After about 20–40 min the suspension turned into a clear solution that was stirred at RT for about 12 h (Scheme 2). Reaction completion was monitored via ^{31}P-NMR spectroscopy. The reaction invariably led to a 1:1 mixture of the mono (**9a-e**) and bis phosphoramidates which were easily separated *via* standard column chromatography on silica gel. Thanks to the easy separation, no further attempts to control the starting substrates ratio in favour of the mono prodrugs were performed. Worth to note at this point is that the phosphoroamidation reactions proceed without stereocontrol and all final prodrugs were obtained as a mixture of four diastereoisomers. Unfortunately, it was not possible to separate the diastereomers via chromatography. Overall, the desired monophosphate prodrugs can be isolated in yields ranging from 21 to 39 %.

2.1.2. Synthesis of fluorescent Fingolimod prodrug

For the synthesis of the fluorescent tagged version of prodrug **9a**[13] we had to prepare the appropriately functionalised Fingolimod derivative **17** (Scheme 3).

The preparation of the fluorescent prodrug started from commercially available 1-(benzyloxy)−4-(2-iodoethyl)benzene (**10**) that was reacted with diethyl acetamido malonate in presence of sodium hydride in DMF solution affording compound **11**. *Via* a sequence of deprotections (diethyl esters / amide) and amine reprotection (*N*-Boc) we obtained compound **12** in 45 % yield over three steps. Benzyl deprotection, via catalytic hydrogenation, almost quantitatively (98 %) led to phenol **13** that was alkylated with *N,N*-dibenzyl-6-bromohexan-1-amine to provide alkyl dibenzylamino- derivative **14**, which was catalytically hydrogenated to compound **15** in 82 % yield. Finally, its reaction with NBD-Cl in presence of DIPEA, MeOH, occurred rapidly (30 min) at room temperature to yield compound **16** in excellent yield (82 %). Boc deprotection under acidic condition led to the NBD-Fingolimod **17**. This compound was transformed into its phosphoramidate prodrug by reaction with phosphorochloridate **8a** in presence of NMI as chloridate activator in THF solution. Although the yield of **18** was not great (25 %) we did not optimise this reaction further. To note, in this particular case, the Grignard method[14] led to substrate decomposition.

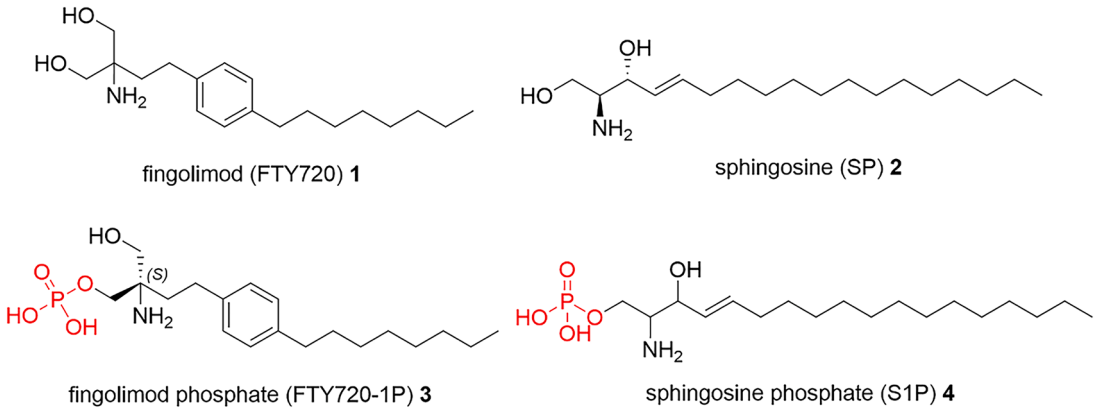

Fig. 1. Structure of Fingolimod 1, the synthetic analogue of sphingosine 2, with their phosphorylated analogues 3 and 4.

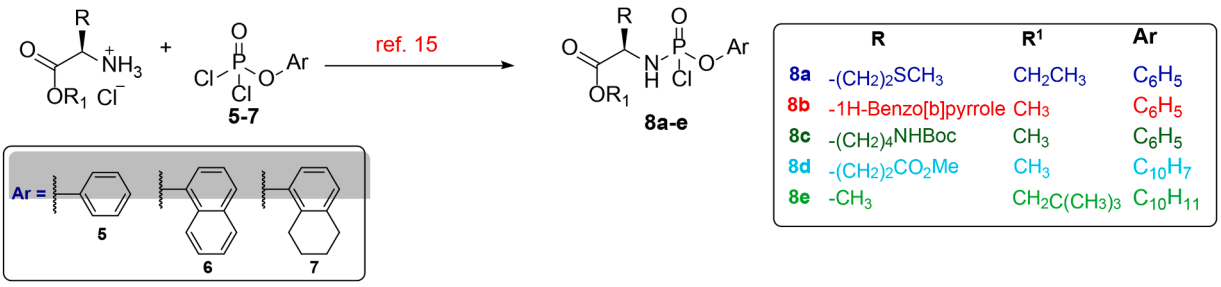

	R	R^1	Ar
8a	$-(CH_2)_2SCH_3$	CH_2CH_3	C_6H_5
8b	-1H-Benzo[b]pyrrole	CH_3	C_6H_5
8c	$-(CH_2)_4NHBoc$	CH_3	C_6H_5
8d	$-(CH_2)_2CO_2Me$	CH_3	$C_{10}H_7$
8e	$-CH_3$	$CH_2C(CH_3)_3$	$C_{10}H_{11}$

Scheme. 1. Preparation of phosphorodichloridate (8a-e).

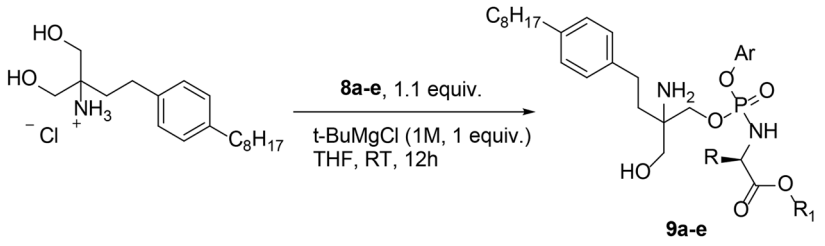

	R	R^1	Ar	yield
9a	$-(CH_2)_2SCH_3$	CH_2CH_3	C_6H_5	37%
9b	-1H-Benzo[b]pyrrole	CH_3	C_6H_5	29%
9c	$-(CH_2)_4NHBoc$	CH_3	C_6H_5	39%
9d	$-(CH_2)_2CO_2Me$	CH_3	$C_{10}H_7$	33%
9e	$-CH_3$	$CH_2C(CH_3)_3$	$C_{10}H_{12}$	21%

Scheme. 2. Preparation of Fingolimod prodrugs via Grignard activation.

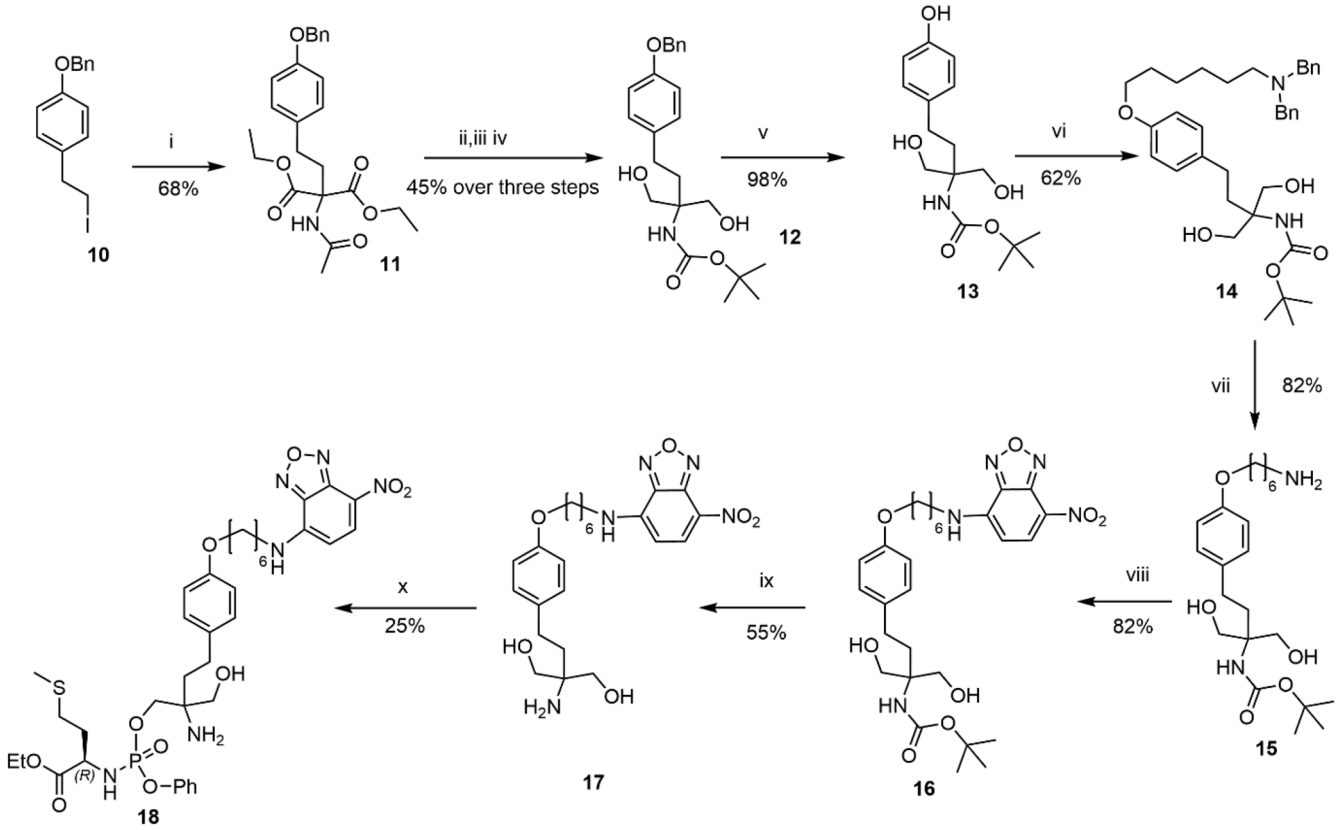

Scheme. 3. Synthesis of fluorescent Fingolimod phosphoramidate derivative (18). Reagents and conditions: (i) diethyl acetamidomalomate, DMF, NaH, 0 °C 3 h, rt 24 h; (ii) $NaBH_4$, $CaCl_2$, EtOH/H_2O, rt, 12 h; (iii) LiOH, THF/MeOH/H_2O 1:2:2 v/v, 5 h, 55 °C; (iv) Boc_2O, DCM, rt, 12 h; (v) H_2, 10 % Pd/C, EtOH/EtOAc 2:1 v/v, rt, 5 h; (vi) N,N-dibenzyl-6-bromohexan-1-amine, K_2CO_3, ACN, reflux, 2.5 h; (vii) H_2, 10 % Pd/C, EtOH/EtOAc 2:1 v/v, rt, 5 h; (viii) NBD-Cl, DIPEA, MeOH, rt, 30 min; (ix) TFA, DCM, 0 °C to rt, 2 h; (x) compound 8a, NMI, THF, 0 °C to rt, 12 h.

3. Prodrug activation studies

The mechanism of activation of phosphoroamidate prodrugs of nucleoside analogues has been studied extensively [11]. Phosphoramidates of fingolimod are believed to follow a similar activation sequence. As depicted in Fig. 2, intracellularly, they are activated by a carboxylic-ester hydrolase or carboxypeptidase-type enzyme which mediated the hydrolysis of the carboxylic ester of the amino acid leading to intermediate **(I)**. The ester cleavage is followed by an internal nucleophilic attack of the acid residue on the phosphorus atom,

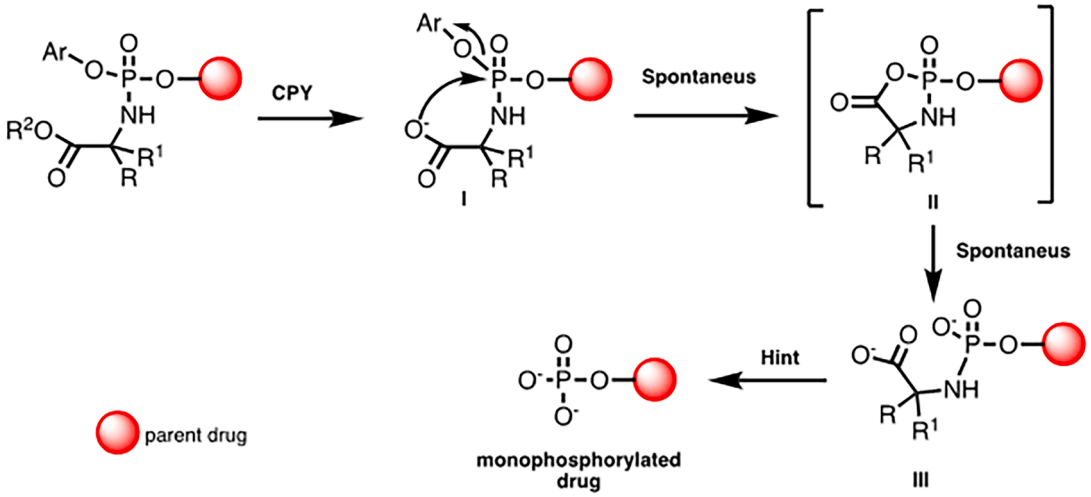

Fig. 2. Putative mechanism of activation of phosphoroamidate prodrug.

displacing the aryloxy group and giving the transient formation of the putative five-membered cyclic intermediate **(II)**. This cyclic anhydride is rapidly hydrolysed to the corresponding aminoacyl phosphoroamidate **(III)** which undergoes P–N bond cleavage, mediated by an enzyme with phosphoramidase activity to eventually release the phosphorylated parent drug. Considering the potential application of these prodrugs for the treatment of neurodegenerative diseases we wanted to evaluate their activation in neuronal cell lysate (compound **9e**).

When prodrug **9e** was subjected to the action of neuronal cell lysate in a mixture of deuterated DMSO and D_2O we indeed observed the activation of the prodrug with the reduction of the intensity of the prodrug peaks at 4 ppm and appearance of a new peak at 1.47 ppm (Fig. 3). Usually, the shift of the peaks toward 1–0 ppm indicates the formation of a monophosphate species. Although the nature of these species was not determined we showed that neural cell lysate can indeed activate our prodrug.

Similar results we obtained for the activation studies of compound **9d** in neuronal cell lysate (Figure S1).

4. Spectroscopic characterisation of prodrug 18

Over the years, various fluorophore scaffolds and novel probes have been developed for application in chemical biology[15] and more specifically for the visualization of membrane bilayer and their interaction with drugs and biomolecules [16]. The green emissive 4-nitroben-z-2-oxa-1,3-diazole (NBD) was selected as suitable fluorescent tag due to its small size, biocompatibility, and its well-known photophysical properties that have so far highlighted its potentiality and versatility

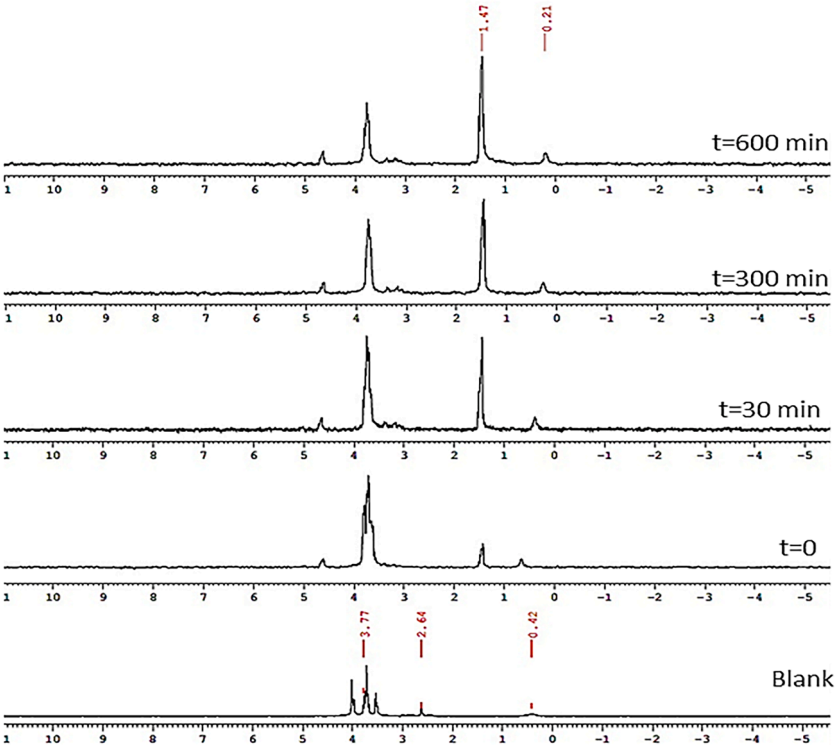

Fig. 3. Overlay of ^{31}P-NMR spectra (202 MHz, DMSO-d6/D_2O) for the activation of Prodrug 9e in neuronal cell lysate at different time points.

[17]. NBD can be indeed considered as an efficient candidate for the development of fluorescent biocompatible sensors[18] and for the functionalization of a plethora of targets like small molecules and biomolecules [19], strengthening its application for chemical biology studies [20]. With our fluorescent labelled prodrug in hand, we set the evaluation of its photophysical properties. The relevant spectroscopic parameters are collected in Table 1.

The obtained values are in accordance with the ones reported for other NBD derivatives [17,22]. The UV–Vis spectrum displays a first band corresponding to a π-π* transition and a second, lower-energy one with a typical charge-transfer character (Fig. 4). The molar extinction coefficients measured in all the tested solvents are in the same order of magnitude (10^3 M^{-1} cm^{-1}) without presenting significant environment-related variations. Fluorescence spectra have a unique band, whose maximum is clearly red shifted by the solvent polarity. Fluorescence quantum yield (Φ_F) strongly decreases in highly polar solvents: from 0.49 in dioxane, it drops to 0.24 in acetonitrile and to 0.12 in methanol. An almost complete quenching effect is observed in water, according to a fluorogenic NBD character.

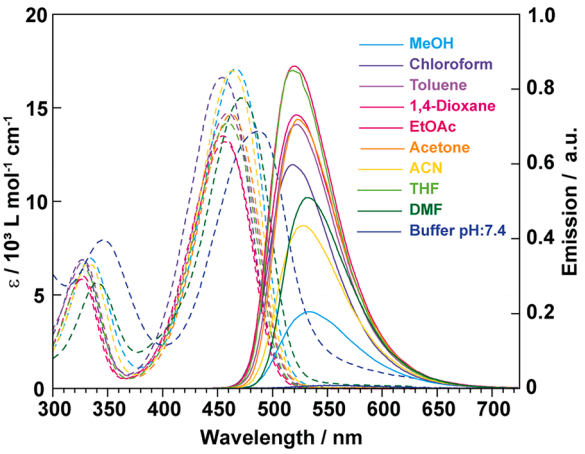

Fig. 4. Absorption (dashed) and emission (solid) spectra of 18 in several solvents. Emission spectra were normalized to 0.1 at excitation wavelength.

4.1. Studies in lipid bilayer membranes

To gain information about the behavior of our prodrugs with respect to biological membranes we set to evaluate the interaction between the prodrug **18** and liposomal bilayer models. Two liposome systems, dipalmitoyl phosphatidylcholine (DPPC) and dioleoyl phosphatidylcholine (DOPC) characterized by different degrees of membrane fluidity were employed. The partitioning kinetic inside the membrane was evaluated by monitoring the variation of fluorescence intensity upon addition of the lipid vesicles (Fig. 5a, b and S2a). Based on the same kinetic assay, dithionite quenching was performed to better understand the location of **18** in the membrane [23]. Upon partitioning time, a solution of sodium dithionite was added to liposomes inducing a remarkable quench of **18** fluorescence signals. The emission intensity signals dropped by 88 and 83 % in DOPC and DPPC respectively and both liposomes were not emissive after five minutes (Figure S3). The final addition of Triton X-100 to the solution to lyse the liposome was depicted by a minor drop of the emission intensity of around 2 %. Since DOPC and DPPC liposomes are not permeable to dithionite, the recorded results were a clear indication of the location of **18** on the outer leaflet of the liposomes [24].

The plot of F/F_0 - where F_0 is the weak emission of the probe in buffer - as a function of time leads to an emission plateau over 40 min for both DOPC and DPPC, indicating that the partitioning process is not immediate. Then, a liposome titration at a constant concentration (8.9 μM) of **18** was conducted (Fig. 5c, d and S2b) to estimate the partition coefficient of the NBD-labelled compound between water and the lipidic vesicles. No significant difference has been found comparing the two model lipids: DOPC partition coefficient - $K_{rip\ DOPC} = 3.9 * 10^5$ – resulted to be slightly higher than its relative DPPC value, $K_{rip\ DPPC} = 9.5 * 10^4$ (Fig. 5d). The observed data can be rationalized by considering the more rigid DPPC structure at room temperature, due to a solid-ordered PC packing arrangement that is subjected to a liquid-disordered transition at 41 °C.

The probe intercalated both into DOPC and DPPC liposomes were warmed up to 55 °C and cooled down to 25 °C, exploring the effect of the membrane phase (Fig. 6). Over the first heating-cooling cycle DOPC showed a decrease of the emission intensity at 55 °C that might be related to both the effect of the temperature on the fluorescence quantum yield of the probe and the higher water content of the membrane due to weaker interactions among the PC molecules at elevated temperature. Cooling down to room temperature was depicted by emission enhancement to a higher intensity compared to the original point which was kept also at the end of the second cycle (Fig. 6a). These might be rationalized by a temperature-induced better partitioning of the probe inside the membrane or a more water-shielded location in the membrane of the bulky fluorogenic **18** upon the temperature cycle. DPPC, instead, showed already a slight emission increase at elevated temperature suggesting and easier higher partition of **18** over the liquid-disordered transition which was confirmed by even more intense emission signal at the end of the first temperature cycle (Fig. 6b). The second heating-cooling step confirmed the data obtained after the first one, indicating that the DPPC phase transition favored the probe intercalation into the membrane and the later recovered more ordered phase below 41 °C did not push out the probe out of the bilayer. It is worth noting that, upon the temperature cycles, the recorded emission intensity signal in DOPC and in DPPC were close suggesting similar and stable partition efficiency of the **18** slightly higher than the values reached by the more canonical equilibration over time.

This experimental evidence can be evaluated as a positive proof of the effective partitioning of the investigated compound in liposome models. Indeed, the presence of NBD fluorophore, already applied for the precise staining of biological membranes with different purposes [25], resulted in this case in a useful redout system to investigate the affinity of **18** towards amphiphilic carrier systems, envisioning the possibility of use similar platforms to deliver the targeted compound. The comparison of the emission signals recorded in liposomes were very close to the ones observed in polar solvents (e.g. MeOH and DMF) confirming the preferential location of **18** at the water-lipid interface region of the membrane rather than in the hydrophobic layer [26]. This behavior, derived by the NBD looping back to the polar head-group region of the phospholipids, is typically reported for phospholipids labelled with NBD on acyl chains [27].

Table. 1
Photophysical properties of **18**.

	λ_{abs} [a]	λ_{em} [a]	Stokes Shift[a]	ε[a]	Φ_F [b]
MeOH	467	534	2.69±0.01	16.10±0.26	0.12±0.02
$CHCl_3$	453	517	2.73±0.01	14.28±0.01	0.37±0.01
Toluene	458	521	2.64±0.04	11.50±0.21	0.46±0.01
Dioxane	454	521	2.83±0.02	12.84±0.08	0.49±0.01
EtOAc	456	519	2.66±0.01	13.50±0.25	0.48±0.02
Acetone	463	524	2.51±0.04	15.60±0.09	0.41±0.01
ACN	464	528	2.61±0.01	15.76±0.07	0.24±0.02
THF	460	518	2.43±0.03	14.34±0.07	0.51±0.02
DMF	471	532	2.43±0.02	15.75±0.09	0.36±0.01
Buffer[c]	489	552	2.33±0.01	15.43±0.11	0.01±0.01

[a] λ_{abs}, λ_{em}, Stokes shift and ε are reported in nm, 10^3 cm^{-1} and 10^3 M^{-1} cm^{-1}, respectively. All photophysical values reflect the average of three independent measurements.

[b] Φ_F was measured referring to Coumarin 153 as standard[21] Φ_F:0.38 in EtOH, λ_{ex} 421 nm). c) The buffer used during the measurements was 100 mM NaCl and 10 mM phosphate (pH = 7.4).

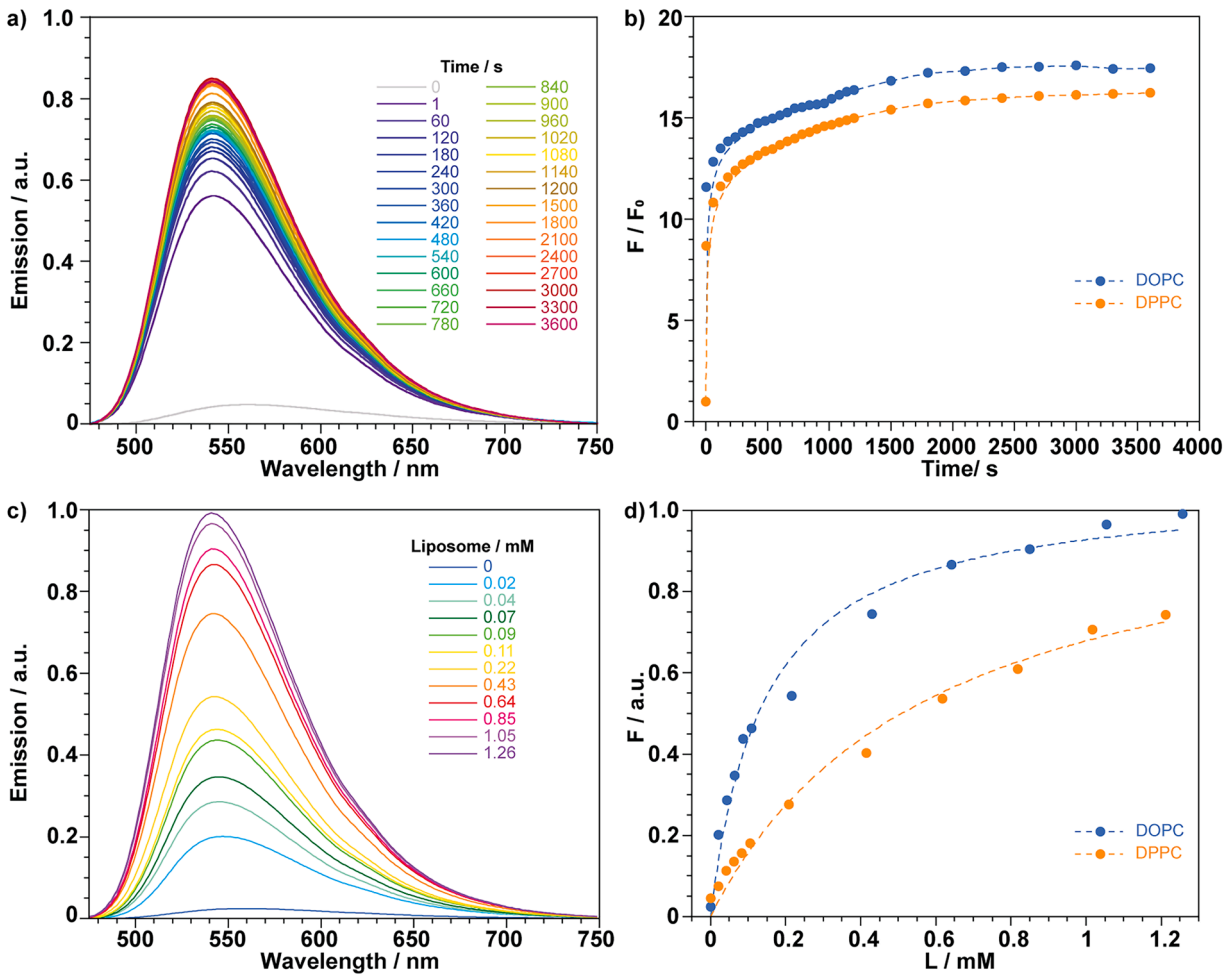

Fig. 5. a) Kinetic intercalation of 18 inside DOPC bilayers, monitored by fluorescence spectroscopy. b) Kinetic intercalation of 18 inside DOPC and DPPC bilayers reported as F/F_0 over time c) 18 emission as a function of DOPC concentration d) 18 emission intensity as a function of the of DOPC and DPPC concentration, the experimental data were fitted with Eq. (2) to evaluate the partition constant in lipid membranes.

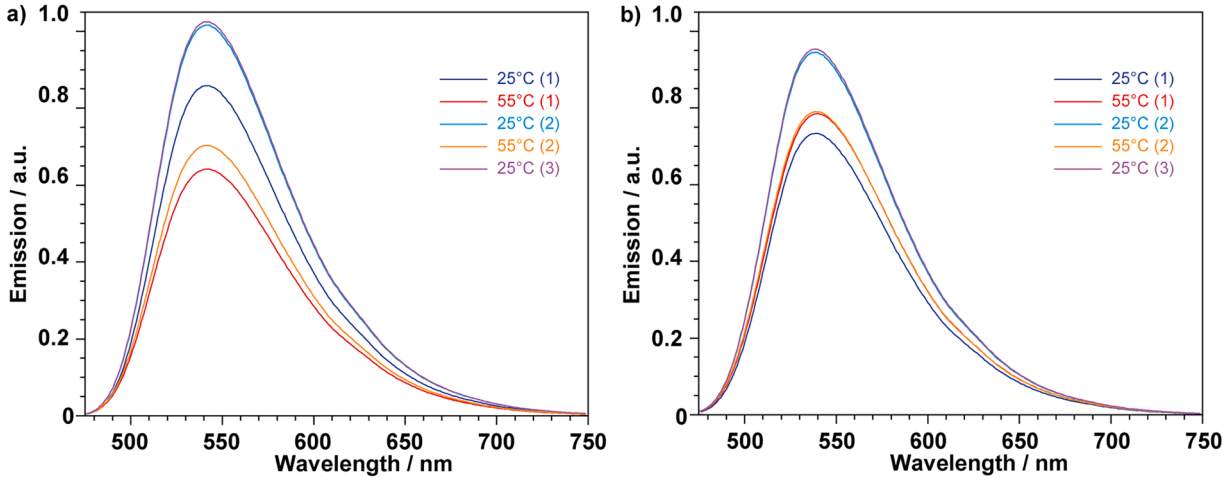

Fig. 6. a) Emission spectra of **18** in DOPC and in b) DPPC at 25 °C, heated at 55 °C, then cooled down to 25 °C, heated to 55 °C and then finally cooled again to 25 °C.

5. Conclusions

In conclusion, we have reported the synthesis of a family of phosphoramidate prodrugs of Fingolimod, a blockbuster drug used in the treatment of MS but also showing interesting activity for the potential treatment of lysosomal disease. We have demonstrated that the other natural amino acids can be successfully installed into the promoiety with a quite simple synthetic strategy giving great flexibility to our methodology. Thanks to the potential use of these prodrugs in the treatment of lysosomal storage diseases such as Niemann-Pick, mucolipidosis IV

we wanted to gather evidence about the distribution/interaction of our prodrug with biological membrane model.

We have therefore successfully prepared a fluorescent tagged prodrug that has been spectroscopically characterized. Our results show that the prodrug can effectively partition into liposome models and therefore it will be plausible to assume that the same behavior will occur with biological membrane such as lysosomes. We believe that the molecules discussed in this study represent a potential treatment for neurodegenerative diseases as well as a research tool for the study of lysosomes in disease.

6. Material & methods

All commercially available chemicals were supplied by either Sigma-Aldrich or Fisher and used without further purification. All solid reagents were dried for several hours under a high vacuum prior to use. For analytical thin-layer chromatography (TLC), precoated aluminium-backed plates (60 F-54, 0.2 mm thickness; supplied by E. Merck AG, Darmstadt, Germany) were used and developed by an ascending elution method. After solvent evaporation, compounds were detected by quenching of the fluorescence, at 254 nm upon irradiation with a UV lamp. Column chromatography purifications were conducted by means of automatic Biotage Isolera One. Fractions containing the product were identified by TLC, pooled and the solvent was removed *in vacuo*. ^{1}H, ^{13}C, ^{31}P-NMR spectra were recorded on a Bruker Avance 500 MHz spectrometer. All ^{13}C and ^{31}P-NMR spectra were proton-decoupled. Chemical shifts are given in parts per million (ppm) and coupling constants (*J*) are measured in Hertz (Hz). The following abbreviations are used in the assignment of NMR signals: s (singlet), d (doublet), m (multiplet), br (broad). The assignment of the signals was done based on the analysis of coupling constants and additional two-dimensional experiments (COSY, HSQC). Analytical High-Performance Liquid Chromatography (HPLC) analysis was performed using Spectra System SCM (with X-select-C18, 5 mm, 4.8 × 150 mm column), Varian Prostar system (LC Workstation-Varian Prostar 335 LC detector). Low resolution mass spectrometry was performed on a Bruker Daltonics MicroTof-LC system (atmospheric pressure ionization, electron spray mass spectroscopy) in positive mode.

6.1. General procedure 1: preparation of phosphoramidating agent 8a-e [14]

To a stirred solution of the appropriate amino acid ester salt (1 equivalent) and the appropriate aryl dichlorophosphate (1 equivalent) in anhydrous CH_2Cl_2 anhydrous Et_3N (2 equivalents) was added dropwise, at −78 °C. Following the addition, the reaction mixture was stirred at −78 °C for 30 min and then at room temperature for 1 h. Formation of the desired compound and disappearance of the starting material was monitored by ^{31}P-NMR. After this period, the solvent was removed under reduced pressure to give an oil. Most of the aryl phosphorochloridates synthesised were purified by flash column chromatography on silica gel (eluting with hexane - ethyl acetate 70:30 v/v). HPLC analysis was performed on a Waters X Select Column 100 Å, 2.5 μm, 4.6 mm X 150 mm, Flow rate: 1 mL/min; under gradient conditions: H_2O/ACN (90:10 v/v) to H_2O/ACN (0:100 v/v) in 30 min. then 5 min. H_2O/ACN (0:100 v/v) and to H_2O/ACN (90:10 v/v) in 2 min with UV detection (254 nm).

6.1.1. Synthesis of phenyl-(ethoxy-l-methioninyl) phosphorochloridate (8a)

Following general procedure 1, the product was obtained in 80 % yield (4.00 g) after purification by flash column chromatography (hexane - ethyl acetate 70:30 v/v). $C_{13}H_{19}ClNO_4P$; M.W: 351.79; ^{1}H NMR ($CDCl_3$, 500 MHz): δ 7.42–7.35 (m, 2H, *ArH*), 7.33–7.24 (m, 3H, *ArH*), 4.64 (t, *J* = 10.4 Hz, 2H, C*H*NH), 4.30 - 4.26 (m, 2H, *CH*$_2$CH$_3$), 2.70–2.54 (m, 2H, *CH*CH$_2$), 2.24–2.13 (m, 2H, *CH*$_2$*S*), 2.10 (s, 3H, SCH$_3$), 1.32 (t, *J* = 7.1 Hz, 2H, *CH*$_2$CH$_3$); ^{31}P NMR ($CDCl_3$, 202 MHz): 8.49, 8.36.

6.1.2. Phenyl-(methoxy-L-tryptophanyl) phosphorochloridate (8b)

Following general procedure 1 the product was obtained in 72 % yield (2.24 g) after chromatography purification (hexane - ethyl acetate 70:30 v/v); $C_{18}H_{18}ClN_2O_4P$; M.W: 392.77; ^{1}H NMR ($CDCl_3$, 500 MHz) δ 8.11 (s, 1H, NH), 7.51–7.44 (m, 1H, *ArH*), 7.32–7.20 (m, 3H, *ArH*), 7.19 (s, 1H, *ArH*), 7.17–6.97 (m, 4H, *ArH*), 4.51–4.30 (m, 1H, *CH*NH), 4.24–4.05 (m, 1H, CH*NH*), 3.61 (s, 3H, OCH$_3$), 3.60 (s, 3H, OCH$_3$), 3.34–3.21 (m, 2H, CH$_2$); ^{31}P NMR (202 MHz, $CDCl_3$) δ 8.08, 7.99.

6.1.3. Phenyl-(methoxy-N-Boc-L-lysinyl) phosphorochloridate (8c)

Following general procedure 1, the product after purification by flash column chromatography (hexane - ethyl acetate 70:30 v/v) was obtained in 89 % yield (2.88 g). $C_{18}H_{28}ClN_2O_6P$; M.W: 674.81; ^{1}H NMR (500 MHz, $CDCl_3$) δ 7.43–7.37 (m, 2H, *ArH*), 7.31–7.25 (m, 3H, *ArH*), 4.59 (d, *J* = 27.6 Hz, 1H, *CH*NH), 4.41–4.27 (m, 1H, CH$_{2a}$*NH*BOC), 4.23–4.05 (m, 1H, CH$_{2b}$*NH*BOC), 3.82 (s, 3H, OCH$_3$), 3.78 (s, 3H, OCH$_3$), 3.12 (d, *J* = 6.6 Hz, 2H, *CH*$_2$CHNHP), 1.90 (m, 1H, CH$_2$), 1.85–1.73 (m, 1H, CH$_2$), 1.57–1.48 (m, 1H, CH$_2$), 1.48 (s, 9H, C(CH$_3$)$_3$); ^{31}P NMR (202 MHz, $CDCl_3$) δ 8.40, 8.28.

6.1.4. Phenyl-(dimethoxy-l-glutamyl) phosphorochloridate (8d)

Following general procedure 1, the product was then purified by flash column chromatography (eluting with hexane - ethyl acetate 70:30 v/v) giving the desired compound in 76 % yield (3.59 g). $C_{15}H_{21}ClNO_6P$; M.W: 377.76; ^{1}H NMR (500 MHz, $CDCl_3$) δ 7.42–7.37 (m, 2H, *ArH*), 7.30–7.26 (m, 3H, *ArH*), 4.50–4.39 (m, 1H, CH*NH*), 4.31–4.18 (m, 1H, *CH*NH), 3.83 (s, 1H, OCH$_3$), 3.81 (s, 1.5H, OCH$_3$), 3.70 (s, 1.5H, OCH$_3$), 3.67 (s, 1.5H, OCH$_3$), 2.64–2.35 (m, 2H, *CH*$_2$CO$_2$Me), 2.32–2.22 (m, 1H, CH*CH*$_2$), 2.13–2.00 (m, 1H, *CH*CH$_2$); ^{31}P NMR (202 MHz, $CDCl_3$) δ 8.34, 8.24.

6.2. General procedure 2: preparation of prodrugs 9a-e

1 M *t*BuMgCl in THF (1 equivalent) was added dropwise to a solution of primary alcohol (e.g., Fingolimod hydrochloride, (1 equivalent) in anhydrous THF (7 mL) under anhydrous conditions. The mixture was stirred at room temperature for one hour. After this time, the appropriate phosphorochloridate (1 equivalent) in anhydrous THF (2 mL) was added dropwise to the stirring reaction mixture. The reaction was left to stir for 24 h and then the solvent was removed *in vacuo* and the desired product was dry-loaded to a column and isolated using flash chromatography (eluting with MeOH/CH_2Cl_2 0:100 v/v increasing to 10:90 v/v).

6.2.1. (2S)-ethyl-2-(((2-amino-2-(hydroxymethyl)-4-(4-octylphenyl) butoxy)(phenoxy)phosphoryl)amino)-4-(methylthio) butanoate (9a)

Following the general procedure 2, the product was isolated in 37 % yield (140 mg) as a mixture of four diastereoisomers (99 % purity, HPLC, 254 nm) using flash chromatography on a Biotage Isolera, eluting with CH$_3$OH/CH_2Cl_2 0:100 v/v increasing to 10:90 v/v). (R_f = 0.36, CH_2Cl_2/CH$_3$OH 95:5 v/v); $C_{32}H_{51}N_2O_6PS$; M W: 622.80; ^{1}H NMR ($CDCl_3$, 500 MHz) δ 7.25–7.21 (m, 2H, pH), 7.17–7.13 (m, 2H, *ArH*), 7.09–7.04 (m, 1H, *ArH*), 7.10–6.96 (m, 4H, *ArH*), 4.16–3.78 (m, 5H, POCH$_2$, O*CH*$_2$CH$_3$, C*H*NH), 3.50–3.17 (m, 2H, *CH*$_2$OH), 2.56–2.33 (m, 6H, CH$_2$C*H*$_2$Ph, *CH*$_2$C$_7$H$_{15}$, *CH*$_2$*S*), 1.98–1.91 (m, 4H, S*CH*$_3$, C*H*$_{2a}$CH$_2$S), 1.87–1.69 (m, 1H, C*H*$_{2b}$CH$_2$S), 1.62–1.50 (m, 6H, C*H*$_2$CH$_2$Ph, C*H*$_2$C$_6$H$_{13}$,), 1.22–1.13 (m, 13H, 5 X CH$_2$, C$_5$*H*$_{10}$CH$_3$, OCH$_2$CH$_3$), 0.80 (m, 3H, CH$_3$). ^{31}P NMR ($CDCl_3$, 202 MHz) δ 4.56, 4.30, 4.24, 3.98; ^{13}C NMR ($CDCl_3$, 125 MHz) δ 172.88, 172.84, 172.79, 172.78, 172.76, 172.74, 150.68, 150.61, 150.56, 140.51, 140.49, 138.99, 138.92, 129.77, 129.73, 128.43, 128.17, 128.15, 128.13, 125.25, 125.21, 125.16, 120.50, 120.46, 120.40, 120.38, 120.36, 120.34, 120.25, 120.21, 69.51, 69.46, 69.36, 69.31, 69.20, 69.16, 65.32, 65.17, 61.80, 61.77, 61.08, 61.03, 58.26, 56.00, 55.84, 53.79, 53.72, 53.52, 53.39, 36.11, 36.05, 35.56, 33.53,

33.48, 33.43, 31.90, 31.59, 29.75, 29.70, 29.65, 29.49, 29.38, 29.27, 28.63, 28.60, 22.67, 15.41, 15.32, 14.25, 14.18, 14.14, 14.11; MS [ES+] *m/z* 623.3 $[M+H]^+$; HPLC t_R = 17.00 min.

6.2.2. *(2S)-methyl-2-(((2-amino-2-(hydroxymethyl)-4-(4-octylphenyl) butoxy)(phenoxy)phosphoryl)amino)-3-(1H-indol-3-yl)propanoate (9b)*

Following the general procedure 2 the desired product was isolated in 29 % yield (110 mg) (95 % purity, HPLC, 254 nm), as a mixture of four diastereoisomers using flash chromatography on a Biotage Isolera, eluting with CH_3OH/CH_2Cl_2 0:100 v/v increasing to 10:90 v/v). (R_f = 0.18, CH_2Cl_2/CH_3OH 95:5 v/v); $C_{37}H_{50}N_3O_6P$; M. W: 663.78; ^1H NMR ($CDCl_3$, 500 MHz) δ 8.49 (bs, 1H, NH), 7.46–7.40 (m, 1H, *ArH*), 7.24 (m, 2H, *ArH*), 7.1–6.88 (m, 1H, 10H), 4.28–4.16 (m, 1H, C*H*NH), 3.94–3.64 (m, 3H, CHN*H*, $POCH_2$), 3.27–3.01 (m, 4H, CH_2OH, CHCH_2), 3.57, 3.56, 3.55, 3.53 (4 s, 3H, OCH_3), 2.51–2.38 (m, 4H, CH_2CH_2Ph, C$H_2C_7H_{15}$), 1.52–1.27 (m, 4H,CH_2CH$_2$Ph, C$H_2C_6H_{13}$), 1.22–1.14 (m, 10H, 2X CH_2, $C_5H_{10}CH_3$), 0.80 (t, *J* = 6.8 Hz, 3H, CH_3); ^{31}P NMR ($CDCl_3$, 202 MHz) δ 4.43, 4.37, 4.19, 4.14; MS [ES+] *m/z* 664.5 $[M+H]^+$. HPLC t_R = 17.20 min.

6.2.3. ***(2R)-methyl-2-(((2-amino-2-(hydroxymethyl)-4-(4-octylphenyl)butoxy)(phenoxy)phosphoryl)amino)-6-((tert-butoxycarbonyl) amino)hexanoate (9c)***

Following the general procedure 2 the desired product was isolated in 39 % yield (160 mg) as a mixture of four diastereoisomers using flash chromatography on a Biotage Isolera, eluting with CH_3OH/CH_2Cl_2 0:100 v/v increasing to 10:90 v/v). (R_f = 0.40, CH_2Cl_2/CH_3OH 95:5 v/v); $C_{37}H_{60}N_3O_8P$; M.W: 705.86; ^1H NMR ($CDCl_3$, 500 MHz) δ 7.35–7.32 (m, 2H, Ph), 7.24–7.22 (m, 2H, Ph), 7.20–7.17 (m, 1H, Ph), 7.12–7.06 (m, 4H, *ArH*), 4.67–4.56 (m, 1H, C*H*NH), 4.06–4.95 (m, 4H, CH_2NH, POCH_2), 3.71, 3.69, 3.68 (3 s, 3H, OCH_3), 3.61–3.42 (m, 2H, CH_2OH), 3.07–3.06 (m, 2H, CH_2CH), 2.64–2.56 (m, 4H, CH_2CH_2Ph, C$H_2C_7H_{15}$), 1.84–1.59 (m, 6H, CH_2CH$_2$NH, CH_2CH$_2$Ph, C$H_2C_6H_{13}$), 1.46 (s, 9H, C$(CH_3)_3$), 1.43–1.39 (m, 2H, CH_2CH$_2$CH), 1.32–1.24 (m, 10H, $C_5H_{10}CH_3$), 0.90 (t, *J* = 6.8 Hz, 3H, CH_3); ^{31}P NMR ($CDCl_3$, 202 MHz) δ 4.56, 4.32, 4.06, 3.86; ^{13}C NMR ($CDCl_3$, 125 MHz) δ 173.67, 173.62, 173.45, 156.05, 150.61, 140.56, 138.91, 129.77, 129.74, 128.67, 128.52, 128.50, 128.44, 128.16, 128.13, 128.10, 128.09, 125.24, 125.20, 125.15, 120.50, 120.46, 120.43, 120.39, 120.37, 120.34, 69.24, 69.08, 65.36, 65.30, 58.41, 54.62, 54.40, 52.49, 50.79, 40.15, 40.08, 36.05, 33.88, 33.84, 33.78, 31.90, 31.60, 29.50, 29.38, 29.28, 28.63, 28.44, 22.68, 22.24, 22.20, 18.44, 14.11; MS [ES+] *m/z* 706.8 $[M+H]^+$.

6.2.4. *Methyl-3-(((2-amino-2-(hydroxymethyl)-4-(4-octylphenyl)butoxy) (naphthalen-1-yloxy)phosphoryl)amino)propanoate (9d)*

Following the general procedure 5.2, the product was isolated in 33 % yield (115 mg) as a mixture of four diastereoisomers (97 % purity, HPLC, 254 nm), using flash chromatography on a Biotage Isolera, eluting with CH_3OH/CH_2Cl_2 0:100 v/v increasing to 10:90 v/v). (R_f = 0.26, CH_2Cl_2/CH_3OH 95:5 v/v); Many signals overlap in ^1H, ^{13}C spectra; $C_{33}H_{47}N_2O_6P$, MW: 598.71; ^1H NMR ($CDCl_3$, 500 MHz) δ 8.06–8.02 (m, 1H, Naph), 7.75–7.74 (m, 1H, Naph), 7.57 (d, *J* = 8.2 Hz, 1H, Naph), 7.45–7.38 (m, 3H, Naph), 7.31–7.29 (m, 1H, Naph), 7.00–6.91 (m, 4H, *ArH*), 3.98–3.79 (m, 2H, $POCH_2$), 3.54 (s, 3H, CH_3), 3.28–3.14 (m, 4H, CH_2OH, CH_2NH), 2.45–2.35 (m, 6H, CH_2CO, CH_2CH_2Ph, C$H_2C_7H_{13}$), 1.57–1.45 (m, 2H, $CH_2C_6H_{13}$), 1.44–1.36 (m, 2H, CH_2CH$_2$Ph), 1.29–1.14 (m, 10H, 5 x CH_2, $C_5H_{10}CH_3$), 0.80–0.78 (m, 3H, CH_3). ^{31}P NMR (202 MHz, $CDCl_3$) δ 6.45, 6.20; ^{13}C NMR ($CDCl_3$, 125 MHz) δ 172.43, 146.55 (d, J_{PH} = 7.5 Hz), 146.53 (d, J_{PH} = 7.5 Hz), 140.49, 140.45, 138.95, 138.90, 134.76, 128.66, 128.42, 128.38, 128.13, 128.10, 127.90, 127.88, 125.65, 125.59, 125.54, 125.45, 125.59, 125.54, 125.07, 125.00, 121.52, 121.49, 115.67 (d, J_{PC} = 2.5 Hz), 115.51, (d, J_{PC} = 2.5 Hz), 69.43, 68.94, 65.35, 65.27, 55.88, 51.82, 37.44, 37.41, 36.08, 35.96, 35.73, 35.56, 31.92, 31.61, 29.51, 29.40, 29.29, 28.59, 28.56, 22.69, 14.13; MS [ES+] *m/z* 599.71 $[M+H]^+$, 621.7 $[M+Na]^+$. HPLC t_R = 18.5 and 19.0 min.

6.2.5. *(2R)-neopentyl-2-(((2-amino-2-(hydroxymethyl)-4-(4-octylphenyl) butoxy)((5,6,7,8-tetrahydronaphthalen-1-yl)oxy)phosphoryl)amino) propanoate (9e)*

Following the general procedure 5.2, the product was isolated in 21 % yield (100 mg) as a mixture of four diastereoisomers (purity 98 %, HPLC, 254 nm), using flash chromatography on a Biotage Isolera, eluting with CH_3OH/CH_2Cl_2 0:100 v/v increasing to 10:90 v/v). (R_f = 0.42, CH_2Cl_2/CH_3OH 95:5 v/v); Many signals overlap in ^1H, ^{13}C spectra; $C_{37}H_{59}N_2O_6P$; MW: 658.85; ^1H NMR ($CDCl_3$, 500 MHz,) δ 7.78–7.05 (m, 7H, *ArH*), 4.33–3.94 (m, 1H, C*H*CH$_3$), 3.94–3.62(m, 4H, $POCH_2$, $CH_2C(CH_3)_3$), 3.45–3.08 (m, 2H, CH_2OH), 2.64–2.61 (4H, m, 2X CH_2 tetrahydronaph), 2.47–2.43 (m, 4H, CH_2CH_2Ph, C$H_2C_7H_{15}$), 1.73 - 1.43 (m, 6H, 2 x CH_2 tetrahydronaph, $CH_2C_6H_{13}$), 1.38–1.31 (m, 2H, CH_2CH$_2$Ph) 1.28–1.09 (m, 10H, 5 x CH_2, $C_5H_{10}CH_3$), 0.85, 0.84, 0.83, 0.83 (4 s, 9H, C$(CH_3)_3$), 0.84 −0.78 (m, 3H, CH_3); ^{31}P NMR ($CDCl_3$, 202 MHz,) δ 4.62, 4.46, 4.23, 4.12; ^{13}C NMR ($CDCl_3$, 125 MHz) δ 173.79, 173.73, 173.68, 173.66, 173.62, 173.60, 148.76, 140.52, 140.51, 139.57, 139.54, 139.50, 138.97, 138.95, 138.87, 128.71, 128.67, 128.62, 128.43, 128.13, 128.10, 128.09, 117.13, 74.81, 65.36, 65.00, 50.48, 50.37, 36.10, 35.98, 35.56, 31.91, 31.60, 31.44, 29.50, 29.47, 29.37, 29.28, 28.61, 28.59, 26.35, 23.55, 23.49, 21.26, 21.22, 21.17, 21.12, 14.11; MS [ES+] *m/z* 659.4 $[M+H]^+$, HPLC t_R = 21.80, 22.70 min.

6.2.6. *Synthesis of diethyl 2-acetamido-2-(4-(benzyloxy)phenethyl)malonate (11) [28]*

Under argon atmosphere, to a stirred solution of diethyl acetamidomalomate (30.7 mmol, 6.67 g) in anhydrous DMF (45 mL) was added NaH (60 % in oil) (57.89 mmol, 0.66 g) at 0 °C and the resulting mixture was stirred for 3 h at the same temperature. To this mixture a solution of 1-(benzyloxy)−4-(2-iodoethyl)benzene (**10**) (5.20 g, 15.36 mmol) in dry DMF (29.5 mL) was added and the reaction stirred at room temperature for 12 h. After quenching with a few drops of MeOH, the crude was concentrated to dryness under vacuum. The mixture was extracted with EtOAc, washed with 1 M HCl, saturated sodium bicarbonate, brine, dried with Na_2SO_4, and concentrated *in vacuo*. The crude product was purified by column chromatography (hexane/EtOAc 70:30) giving pure diethyl 2-acetamido-2-(4-(benzyloxy)phenethyl)malonate (**10**) as white powder, in 72 % yield (4.73 g). ^{1H}NMR (500 MHz, $CDCl_3$): δ_H 7.41 (d, *J* = 9.0 Hz, 2H, *HBn*), 7.36 (t, *J* = 7.2 Hz, 2H, *HBn*), 7.32–7.28 (m, 1H, *HBn*), 7.04 (d, *J* = 8.7 Hz, 2H, *ArH*), 6.87 (d, *J* = 8.7 Hz, 2H, *ArH*), 6.74 (1H, N*H*), 5.03 (s, 2H, OCH_2Ph), 4.24–4.13 (m, 4H, OCH_2CH_3), 2.66–2.63 (m, 2H, CH_2CH_2I), 2.43–2.40 (m, 2H, CH_2CH_2I), 1.97 (s, 3H, NHCOCH_3) 1.23 (t, *J* = 7.2 Hz, OCH$_2CH_3$) ppm; MS (ES+): *m/z* = 450.18 $[M+Na]^+$.

6.2.7. *Synthesis of tert-butyl(4-(4-(benzyloxy)phenyl)−1-hydroxy-2-(hydroxymethyl)butan-2-yl)carbamate (12) [28]*

To a solution of diethyl 2-acetamido-2-(4-(benzyloxy)phenethyl) malonate (**11**) (2.14 g, 4.9 mmol,) in 60 mL of EtOH/H_2O (2:1) was added $CaCl_2$ (12.5 mmol, 1.39 g) followed by the addition of $NaBH_4$ (24.9 mmol, 945 mg) by portion. The mixture was stirred overnight at room temperature and was then quenched at 0 °C with MeOH added dropwise and concentrated to dryness under vacuum. The crude was extracted with EtOAc and washed with 1 M HCl, saturated sodium bicarbonate solution, brine, dried with Na_2SO_4, filtered, and concentrated *in vacuo*. The crude was purified by chromatography (hexane/EtOAc 70:30) giving the pure product *N*-(4-(4-(benzyloxy)phenyl)−1-hydroxy-2-(hydroxymethyl)butan-2-yl)acetamide as white powder in 72 % yield (3.18 g). ^{1H}NMR (500 MHz, MeOD): δ_H 7.42 (d, *J* = 8.5 Hz, 2H, *HBn*), 7.35 (t, *J* = 7.2 Hz, 2H, *HBn*), 7.29 (t, *J* = 7.2 Hz, 1H, *HBn*), 7.11 (d, *J* = 8.7 Hz, 2H, *ArH*), 6.88 (d, *J* = 8.7 Hz, 2H, *ArH*), 5.04 (s, 2H, OCH_2Ph), 3.76 (d, *J* = 11.3 Hz, 2H, CH_2OH), 3.67 (d, *J* = 11.2 Hz, 2H, CH_2OH), 2.56–2.52 (m, 2H, PhCH_2CH_2), 1.97–1.94 (m, 5H, PhCH_2CH_2 and NHCOCH_3) ppm; MS (ES+): *m/z* = 366.18 $[M+Na]^+$. This compound (1.9 mmol, 0.64 g) was dissolved in THF/MeOH/H_2O (1:2:2) (5 mL / 10 mL / 10 mL) and to the solution was added lithium hydroxide (15.2

mmol, 0.36 g) at room temperature and the rusting mixture was stirred at 55 °C for 5 h. The reaction mixture was then extracted with EtOAc and washed with brine, dried with Na_2SO_4, filtered, and concentrated *in vacuo*. The product was isolated as white powder, used for the next reaction without further purification. 84 %, 0.48 g. ^{1}HNMR (500 MHz, $CDCl_3$): δ_H 7.42 (d, $J = 7.0$ Hz, 2H, *HBn*), 7.37 (t, $J = 7.2$ Hz, 2H, *HBn*), 7.33–7.29 (m, 1H, *HBn*), 7.10 (d, $J = 8.7$ Hz, 2H, *ArH*), 6.89 (d, $J = 8.7$ Hz, 2H, *ArH*), 5.03 (s, 2H, OCH_2Ph), 3.59 (d, $J = 10.7$ Hz, 2H, CH_2OH), 3.49 (d, $J = 10.7$ Hz, 2H, CH_2OH), 2.61–2.57 (m, 2H, PhCH_2CH_2), 1.69–1.66 (m, 2H, PhCH$_2CH_2$) ppm. MS (ES+): $m/z = 324.17$ $[M+Na]^+$. To a solution of 2-amino-2-(4-(benzyloxy)phenethyl)propane-1,3-diol (17.8 mmol, 5.35 g) in DCM (308 mL) was added Boc_2O (44.1 mmol, 6.95 mL) and the mixture was stirred overnight at room temperature. The reaction mixture was concentrated under vacuum and purified by silica gel column chromatography (CH_2Cl_2/MeOH 97:3) giving the pure product as white powder *tert*-butyl(4-(4-(benzyloxy)phenyl)−1-hydroxy-2-(hydroxymethyl)butan-2-yl)carbamate **12** as white powder, (42 %, 3.00 g). ^{1}HNMR (500 MHz, $CDCl_3$): δ_H 7.42 (d, $J = 7.3$ Hz, 2H, *HBn*), 7.37 (t, $J = 7.3$ Hz, 2H, *HBn*), 7.31 (t, $J = 7.2$ Hz, 1H, *HBn*), 7.10 (d, $J = 8.5$ Hz, 2H, *ArH*), 6.89 (d, $J = 8.5$ Hz, 2H, *ArH*), 5.02 (s, 2H, OCH_2Ph), 3.85 (d, $J = 11.3$ Hz, 2H, CH_2OH), 3.62 (d, $J = 11.3$ Hz, 2H, CH_2OH), 2.57–2.54 (m, 2H, PhCH_2CH_2), 1.88–1.84 (m, 2H, PhCH$_2$CH_2), 1.45 (s, 9H, O*t*Bu) ppm; MS (ES+): $m/z = 424.50$ $[M+Na]^+$.

6.2.8. *Synthesis of tert-butyl (1-hydroxy-2-(hydroxymethyl)-4-(4-hydroxyphenyl)butan-2-yl)carbamate (13)*

Under inert atmosphere, to a solution of *tert*-butyl(4-(4-(benzyloxy)phenyl)−1-hydroxy-2-(hydroxymethyl)butan-2-yl)carbamate (**12**) (6.7 mmol, 2.98 g) in EtOH/EtOAc (2:1) (70 mL: 35 mL) was added 10 % Pd/C and subsequently hydrogen gas. The resulting mixture was stirred at room temperature for 5 h. The crude was filtered and concentrated *in vacuo* giving 2.04 g of colorless oil (98 %). The product was used for the next reaction without further purification.^{1}HNMR (500 MHz, $CDCl_3$): δ_H 7.01 (d, $J = 8.5$ Hz, 2H, *ArH*), 6.72 (d, $J = 8.5$ Hz, 2H, *ArH*), 5.02 (s, 2H, OCH_2Ph), 3.85 (d, $J = 11.5$ Hz, 2H, CH_2OH), 3.61 (d, $J = 11.5$ Hz, 2H, CH_2OH), 2.55–2.52 (m, 2H, PhCH_2CH_2), 1.86–1.82 (m, 2H, PhCH$_2CH_2$), 1.44 (s, 9H, O*tBu*) ppm; MS (ES+): $m/z = 334.17$ $[M+Na]^+$.

6.2.9. *Synthesis of tert-butyl (4-(4-((6-(dibenzylamino)hexyl)oxy)phenyl)−1-hydroxy-2-(hydroxymethyl)butan-2-yl)carbamate (14)*

To a solution of *tert*-butyl (1-hydroxy-2-(hydroxymethyl)−4-(4-hydroxyphenyl)butan-2-yl)carbamate (**13**) (2.1 mmol, 0.65 g) in dry ACN (7.9 mL) was added anhydrous potassium carbonate (3.1 mmol, 0.44 g) followed by the addition of a solution of *N,N*-dibenzyl-6-bromohexan-1-amine [29] (3.1 mmol, 1.11 g) in dry ACN (7.75 mL). The mixture was heated at reflux for 2 h. The crude was concentrated *in vacuo* and then extracted with EtOAc, dried with Na_2SO_4, filtered, and concentrated *in vacuo*. The mixture then was purified by silica gel column chromatography (EtOAc/hexane 8:2) and the product was obtained as colorless oil in 62 % yield (0.77 g); ^{1}HNMR (500 MHz, $CDCl_3$): δ_H 7.36 (d, $J = 7.1$ Hz, 4H, *HBn*), 7.30 (t, $J = 7.3$ Hz, 4H, *HBn*), 7.24 (t, $J = 7.3$ Hz, 2H, *HBn*), 7.09 (d, $J = 8.6$ Hz, 2H, O-*ArH*), 6.80 (d, $J = 8.5$ Hz, 2H, O-*ArH*), 3.87 (d, $J = 6.6$ Hz, 2H, OCH_2CH_2), 3.83 (d, $J = 11.5$ Hz, 2H, CH_2OH), 3.61 (d, $J = 11.5$ Hz, 2H, CH_2OH), 3.55 (s, 4H, NCH_2Ph), 2.57–2.54 (m, 2H, PhCH_2CH_2), 2.42 (t, $J = 7.1$ Hz, 2H, NCH_2CH_2), 1.88–1.85 (m, 2H, PhCH$_2CH_2$), 1.75–1.69 (m, 2H, $CH_2CH_2CH_2$), 1.57–1.50 (m, 2H, $CH_2CH_2CH_2$), 1.46 (s, 9H, O*tBu*), 1.37–1.31 (m, 4H, $CH_2CH_2CH_2$) ppm. MS (ES+): $m/z = 613.81$ $[M+Na]^+$

6.2.10. *tert-butyl(4-(4-((6-aminohexyl)oxy)phenyl)-1-hydroxy-2-(hydroxymethyl)butan-2-yl)carbamate (15)*

Under inert atmosphere, to a solution of *tert*-butyl (4-(4-((6-(dibenzylamino)hexyl)oxy)phenyl)−1-hydroxy-2-(hydroxymethyl)butan-2-yl)carbamate (**14**) (1.3 mmol, 0.77 g) in EtOH/EtOAc (2:1) (16.25 mL: 8.13 mL) was added 10 % Pd/C and subsequently hydrogen gas. The resulting mixture was stirred at room temperature for 5 h. The crude was filtered and concentrated *in vacuo* giving a colorless oil as product. The product was used for the next reaction without further purification. Colorless oil, 82 %, 0.44 g. ^{1}HNMR (500 MHz, $CDCl_3$): δ_H 7.08 (d, $J = 8.6$ Hz, 2H, O-*ArH*), 6.78 (d, $J = 8.5$ Hz, 2H, O-*ArH*), 5.08 (br, 1H, N*H*CO) 3.90 (t, $J = 6.5$ Hz, 2H, OCH_2CH_2), 3.83 (d, $J = 11.4$ Hz, 2H, CH_2OH), 3.60 (d, $J = 11.5$ Hz, 2H, CH_2OH), 2.68 (t, $J = 7.0$ Hz, 2H, NHCH_2CH_2), 2.56–2.53 (m, 2H, PhCH_2CH_2), 1.87–1.83 (m, 2H, PhCH$_2CH_2$), 1.78–1.71 (m, 2H, $CH_2CH_2CH_2$), 1.49–1.41 (m, 13H, $CH_2CH_2CH_2$, $CH_2CH_2CH_2$ and O*tBu*), 1.39–1.34 (m, 4H, $CH_2CH_2CH_2$) ppm; MS (ES+): $m/z = 423.56$ $[M+Na]^+$

6.2.11. *tert-butyl(1-hydroxy-2-(hydroxymethyl)−4-(4-((6-((7-nitrobenzo[c][1,2,5]oxadiazol-4-yl)amino)hexyl)oxy)phenyl)butan-2-yl)carbamate (16)*

To a solution of *tert*-butyl(4-(4-((6-aminohexyl)oxy)phenyl)−1-hydroxy-2-(hydroxymethyl)butan-2-yl)carbamate (**15**) (0.24 mmol, 0.10 g) in MeOH (2.4 mL) were added consequently *N,N*-diisopropylethylamine (0.48 mmol, 84 μL) and 4-chloro-7-nitrobenzofurazan (NBD-Cl) (0.24 mmol, 0.05 g) and the resulting mixture was stirred at room temperature for 30 min. The crude was evaporated *in vacuo* and the residue was purified by silica gel column chromatography (DCM/MeOH 95:5) to afford the product as dark orange powder, 82 %, 0.44 g. ^{1}HNMR (500 MHz, $CDCl_3$): δ_H 8.46 (d, $J = 8.6$ Hz, 2H, H—NBD), 7.07 (d, $J = 8.6$ Hz, 2H, O-*ArH*), 6.77 (d, $J = 8.7$ Hz, 2H, O-*ArH*), 6.36 (br, 1H, N*H*—NBD), 6.16 (d, $J = 8.6$ Hz, 2H, *H*—NBD), 5.06 (br, 1H, N*H*CO), 3.94 (t, $J = 6.2$ Hz, 2H, OCH_2CH_2), 3.88–3.85 (m, 2H, CH_2OH), 3.65–3.61 (m, 2H, CH_2OH), 3.55–3.43 (m, 2H, NHCH_2CH_2), 2.57–2.54 (m, 2H, PhCH_2CH_2), 1.87–1.78 (m, 6H, PhCH$_2CH_2$, $CH_2CH_2CH_2$ and $CH_2CH_2CH_2$), 1.60–1.53 (m, 4H, $CH_2CH_2CH_2$ and $CH_2CH_2CH_2$), 1.45 (m, 9H, CH_3, *t*Bu) ppm. ^{13}C NMR (125 MHz, MeOD): δ_C 157.25 (NHC=O), 156.47 (C—NBD), 144.27 (C—NBD), 143.90 (C—NBD), 136.51 (CH—NBD), 133.79 (“*ipso*” OPh), 129.19 (C*ArH*), 123.97 (C-Ph), 114.49 (C*ArH*), 98.52 (CH—NBD), 70.61 (OC*t*Bu), 67.55 (OCH_2CH_2), 66.49 (CH_2OH), 53.44 (CH_2CCH_2), 43.85 (NHCH_2CH_2), 35.31 (PhCH$_2$CH_2), 29.06 ($CH_2CH_2CH_2$), 28.62 ($CH_2CH_2CH_2$), 28.47 (PhCH_2CH_2), 28.34 (CH_3, *t*Bu), 26.62 ($CH_2CH_2CH_2$), 25.77 ($CH_2CH_2CH_2$) ppm.

$$MS(ES+): m/z = 596.65[M + Na]^+$$

6.2.12. *2-amino-2-(4-((6-((7-nitrobenzo[c][1,2,5]oxadiazol-4-yl)amino)hexyl)oxy)phenethyl)propane-1,3-diol (17)*

Carbamate (**16**) (0.53 mmol, 0.30 g) was solubilized in DCM (18 mL) and the reaction mixture was cooled down to 0 °C followed by the addition of trifluoroacetic acid (1.66 mL). After 10 min, the reaction was allowed to reach room temperature and stirred for 2 h. The crude was evaporated *in vacuo* and the residue was purified by silica gel column chromatography (DCM/MeOH 95:5) to afford the product **17** as bright orange powder in 55 % yield (0.16 g); ^{1}HNMR (500 MHz, $CDCl_3$): δ_H 8.45 (d, $J = 8.7$ Hz, 2H, H—NBD), 7.04 (d, $J = 8.6$ Hz, 2H, O-*ArH*), 6.76 (d, $J = 8.8$ Hz, 2H, O-*ArH*), 6.34 (br, 1H, *NH*—NBD), 6.15 (d, $J = 8.7$ Hz, 2H,*H*—NBD), 3.96–3.91 (m, 4H, OCH_2CH_2 and CH_2OH), 3.74–3.70 (m, 4H, CH_2OH and NHCH_2CH_2), 3.53–3.48 (m, 2H, $CH_2CH_2CH_2$), 2.56–2.53 (m, 2H, PhCH_2CH_2), 2.00–1.97 (m, 2H, PhCH$_2CH_2$), 1.86–1.77 (m, 4H, $CH_2CH_2CH_2$ and $CH_2CH_2CH_2$), 1.56–1.55 (m, 2H, $CH_2CH_2CH_2$) ppm. ^{13}C NMR (125 MHz, MeOD): δ_C 157.45 (C—NBD), 144.39 (C—NBD), 144.07 (C—NBD), 144.00 (C—NBD), 136.73 (CH—NBD), 133.08 (“*ipso*” O-*ArH*), 129.28 (C*ArH*), 124.02 (C-pH), 114.72 (C*ArH*), 98.69 (CH—NBD), 67.67 (OCH_2CH_2), 65.65 (CH_2OH), 58.65 (CH_2CCH_2), 43.93 (NHCH_2CH_2), 33.60 (PhCH$_2$CH_2), 29.23 ($CH_2CH_2CH_2$), 28.68 ($CH_2CH_2CH_2$), 28.58 (PhCH_2CH_2), 26.64 ($CH_2CH_2CH_2$), 25.83 ($CH_2CH_2CH_2$) ppm; MS (ES+): $m/z = 496.23$ $[M+Na]^+$

6.2.13. *Ethyl ((2-amino-2-(hydroxymethyl)−4-(4-((6-((7-nitrobenzo[c][1,2,5]oxadiazol-4-yl)amino)hexyl)oxy)phenyl)butoxy)(phenoxy)phosphoryl)-d-methioninate (18)*

Under inert atmosphere to a solution of 2-amino-2-(4-((6-((7-nitrobenzo[*c*][1,2,5]oxadiazol-4-yl)amino)hexyl)oxy)phenethyl)propane-1,3-diol (**17**) (0.11 mmol, 0.05 g) in anhydrous THF (645 μL) was added ethyl (chloro(phenoxy)phosphoryl)-*l*-methioninate (**8a**) dropwise at room temperature. Consequently, N-methyl imidazole (NMI) was added to the resulting solution and the mixture was stirred at 45°C overnight. The solvent was evaporated under vacuum and the crude was purified by silica gel column chromatography (DCM/MeOH 95:5) to afford the product as bright orange powder; 25 %, 0.02 g. ^{31}P-NMR (202 MHz, $CDCl_3$, mixture of R_P and S_P diastereoisomers): δ_P 4.59, 4.32, 4.22, 4.03 ppm (int, 1:0.6:0.6:0.5). ^{1H}NMR (500 MHz, $CDCl_3$): δ_H 8.45 (d, J = 8.6 Hz, 2H, *H*—NBD), 7.29–7.13 (m, 5H, *ArH*), 7.00 (d, J = 8.4 Hz, 2H, pH), 6.74 (d, J = 8.3 Hz, 2H, *ArH*), 6.56 (br, 1H, N*H*—NBD), 6.15 (d, J = 8.6 Hz, 2H, *H*—NBD), 4.21–4.39 (m, 7H, O*CH*$_2$CH$_3$, NHC*H*CO, O*CH*$_2$CH$_2$ and *CH*$_2$OH), 3.93–3.91 (m, 2H, *CH*$_2$OH), 3.51–3.47 (m, 2H, NHCH$_2$CH$_2$), 2.59–2.39 (m, 4H, *CH*$_2$SCH$_3$ and PhCH$_2$CH$_2$), 2.09 (s, 3H, CH$_2$S*CH*$_3$), 2.04–1.98 (m, 4H, PhCH$_2$*CH*$_2$ and CH*CH*$_2$CH$_2$), 1.84–1.78 (m, 4H, CH$_2$*CH*$_2$CH$_2$ and CH$_2$*CH*$_2$CH$_2$), 1.59–1.52 (m, 4H, CH$_2$*CH*$_2$CH$_2$ and CH$_2$*CH*$_2$CH$_2$), 1.25–1.17 (m, 3H, OCH$_2$*CH*$_3$) ppm. ^{13}C NMR (125 MHz, MeOD): δ_C 175.68–173.15–172.78 (C═O ester), 157.24 (C—NBD), 150.57 (d, ^2J=7.0 Hz, "*ipso*" PO-Ph), 144.28–143.95 (C—NBD), 136.54 (CH—NBD), 133.70–133.60–133.46 ("*ipso*" OPh, C-Ar), 129.79–129.76–129.74–129.12–129.19–125.25–120.49 (d, ^3J=4.5 Hz)–120.44–120.32 (d, ^3J=4.7 Hz)–120.23 (d, ^3J=4.5 Hz)–114.43 (CH-Ar), 98.54 (CH—NBD), 67.67–61.83–61.06 (OCH$_2$CH$_2$, *CH*$_2$OH and OCH$_2$CH$_3$), 53.89–53.76–53.53–53.76 (NHCHCO), 52.81 (CH$_2$CCH$_2$), 43.89 (NHCH$_2$CH$_2$), 33.95–33.43 (d, ^2J=5.9 Hz)–33.31 (d, ^2J=5.9 Hz)–30.49–29.73–29.65–29.09–28.46–28.11–26.67–25.78 (CH$_2$), 15.41–15.31–15.27–15.24 (SCH$_3$), 14.24–14.17–14.11–14.09 (OCH$_2$CH$_3$) ppm.

7. Prodrug activation study in neuronal cell lysate

4 mg of prodrug **9e** are dissolved in a mixture of 150 μL of DMSO-d6 and 100 μL D_2O. The solution is transferred into an NMR tube. The ^{31}P spectrum is recorded (64 scans). To the blank sample in the NMR tube 150 μL of B95a cell lysate (6.000.000 cell/mL) are added and then ^{31}P spectra are recorded at 37 °C (512 scans, 600 s delay, 20 experiments).

8. Spectroscopic characterization

8.1. General

Stock solutions in DMSO of **18** was prepared with a concentration of 1.8 mM. This concentration was then adjusted to have an absorbance between 0.1 and 1 to evaluate the photophysical properties in different organic solvents (molar extinction coefficient, Abs_{max}, Em_{max}). Absorption spectra were recorded with a Shimadzu UV-1900i UV–Vis Spectrophotometer setting the slit at 0.5 nm and using a resolution of 0.5 nm. Steady state emission spectra were measured on a Shimadzu RF-6000 Spectro Fluorophotometer. The excitation and the emission slits were set at 2.5 nm for photophysical measurements, the resolution at 1 nm and the integration time 0.1 s.

8.2. Fluorescence quantum yield evaluation

The above-mentioned stock solution was diluted to have an absorbance lower than 0.1 at excitation wavelength. The fluorescence quantum yield was evaluated compared to an external standard, Coumarine 153 (φ = 0.38 in EtOH, λ_{ex} 421 nm) by applying the following equation:

$$\phi = \phi_{STD}\frac{I}{I_{STD}}\frac{Abs_{STD}}{Abs}\frac{n^2}{n^2_{STD}} \quad (1)$$

Where Φ_{STD} is the fluorescence quantum yield of the standard, I and I_{STD} are the integrated area of the emission band of the sample and the standard, respectively. Abs and Abs_{STD} are the absorbance at the excitation wavelength for the sample and the standard, respectively. n and n_{STD} are the solvent refractive index of the sample and the standard solutions, respectively.

9. Studies in lipid bilayer membranes

9.1. General

Aqueous buffer solutions were prepared with de-ionized water (Millipore RiOs 3 Water System), sodium phosphate monobasic monohydrate, di-sodium hydrogen phosphate dihydrate and sodium chloride (biological grade) properly adjusted to have a final buffer with composition: 10 mM phosphate, 100 mM NaCl, pH 7.4. 1,2-dioleoyl-sn-glycero-3-phosphocholine (DOPC) and 1,2-dipalmitoyl-sn-glycero-3-phosphocholine (DPPC) were purchased from Avanti Polar Lipids. Steady state emission spectra were measured on a Shimadzu RF-6000 Spectro Fluorophotometer. The excitation slit was set at 5 nm and the emission one at 10, the resolution at 1 nm and the integration time 0.1 s.

9.2. DOPC LUVs preparation

A lipid film was prepared by a slow rotary evaporation (30 °C) of a DOPC (25.0 mg, 0.03 mmol) solution in 2 mL of MeOH/$CHCl_3$ 1:1 and a final draining (5 h) *in vacuo*. The obtained film was hydrated with 1.0 mL buffer (10 mM phosphate, 100 mM NaCl, pH 7.4) for 30 min at rt, subjected to freeze-melt cycles (7x, liquid N_2, 40 °C water bath) and extrusions (17x) through a polycarbonate membrane (pore size 100 nm) at rt. Final conditions: 32 mM DOPC, 10 mM phosphate, 100 mM NaCl, pH 7.4. The vesicles were used within one week from the extrusion.

9.3. DPPC LUVs preparation

A lipid film was prepared by a slow rotary evaporation (40 °C) of a DPPC (22.5 mg, 0.03 mmol) solution in 2 mL of MeOH/$CHCl_3$ 1:1 and a final draining (5 h) *in vacuo*. The obtained film was hydrated with 1.0 mL buffer (10 mM phosphate, 100 mM NaCl, pH 7.4) for 30 min at 55 °C, subjected to freeze-melt cycles (7x, liquid N_2, 55 °C water bath) and extrusions (21x) through a polycarbonate membrane (pore size 100 nm) at rt. Final conditions: 31 mM DPPC, 10 mM phosphate, 100 mM NaCl, pH 7.4. The vesicles were used within one week from the extrusion.

9.4. Time dependence measurements (DOPC, DPPC)

In a typical procedure, to a 2900 μL buffer (10 mM phosphate, 100 mM NaCl, pH 7.4 at rt) in a quartz cuvette, DOPC LUVs (100 μL, 1.05 mM DOPC final concentration) or DPPC LUVs (100 μL, 1.02 mM DPPC final concentration) and the prodrug **18** (15 μL, 1.8 mM, 8.9 μM final concentration) were added.

Each solution was mixed at rt and monitored acquiring the emission spectra every 1minute during the first 20 min, then after 5minutes up to 1 h.

9.5. Emission quenching assay (DOPC, DPPC)

In a typical procedure, to a 2900 μL buffer (10 mM phosphate, 100 mM NaCl, pH 7.4 at rt) in a quartz cuvette, the prodrug **18** (15 μL, 1.8 mM, 8.9 μM final concentration) were added and the emission intensity was monitored (λ_{exc} = 455 nm λ_{em}= 550 nm) every 30 s for 5 min. DOPC LUVs (100 μL, 1.05 mM DOPC final concentration) or DPPC LUVs (100 μL, 1.02 mM DPPC final concentration) were added monitoring the emission signal every 2 min for 40 min to reach a plateau in intensity. A solution of sodium dithionite (25 μL of 1 M dithionite, pH 10) was added recording the signal every 15 s for 25 min before lysing the liposomes by

adding a Triton X-100 solution (10 μL, 10 % in water) and registering the emission every 15 s for 10 min.

9.6. Partition coefficient (DOPC, DPPC)

In a typical procedure, different DOPC or DPPC (32 mM or 31 mM respectively) aliquots were added to a solution of prodrug **18** (15 μL, 1.8 mM) in buffer (2.90 mL,10 mM phosphate, 100 mM NaCl, pH 7.4 at rt). The fluorescence spectra were recorded at equilibrium after addition of lipids (25 min for all the vesicles). Then, the maximum intensity (F) was plotted against the lipid concentration (L) for each prepared solution, according to the Eq. (2), reported by Huang [30].

$$F = \frac{F_0 L}{\frac{55.6}{K_{rip}} + L} \quad (2)$$

where F_0 is the maximum fluorescence resulting from the total probe incorporation into membrane and K_{rip} is the partition coefficient.

9.7. Temperature dependent measurements (DOPC, DPPC)

Following a typical procedure to a 2.9 mL buffer solution (10 mM phosphate, 100 mM NaCl, pH 7.4 at rt) in a quartz cuvette, DOPC LUVs (100 μL, 1.05 mM DOPC final) or DPPC LUVs (100 μL, 1.02 mM DPPC final) and the prodrug **18** (15 μL, 1.8 mM, 8.9 μM final) were added. The resulting solution was mixed at room temperature and the emission spectrum was acquired after the equilibration time (60 min for DOPC, 100 min for DPPC). The solution was maintained at 25 ± 1 °C for 15 min before the spectra acquisition (λ_{ex} = 455 nm), the cuvette was then warmed to 55 ± 1 °C and the solution was stored at this temperature for 15 min before the spectra acquisition. The temperature was then lowered down to 25 ± 1 °C and the spectra were acquired after 15 min. The here described temperature cycle was repeated, collecting a total of five measurements for both DOPC and DPPC vesicles (Fig. 6). Data reflect the average of three independent measurements.

CRediT authorship contribution statement

Fabrizio Pertusati: Writing – review & editing, Writing – original draft, Project administration, Investigation, Conceptualization. **Michaela Serpi:** Writing – review & editing, Data curation. **Chiara Morozzi:** Data curation. **Edward James:** Writing – review & editing, Data curation. **Giacomo Renno:** Writing – original draft, Formal analysis, Data curation. **Francesca Cardano:** Writing – original draft, Formal analysis, Data curation. **Andrea Fin:** Writing – review & editing, Supervision.

Declaration of competing interest

The authors declare the following financial interests/personal relationships which may be considered as potential competing interests: Fabrizio Pertusati and Edward James, report financial support was provided by Life Sciences Research Network Wales. Fabrizio Pertusati and Edward James have patent #11078221 issued to UNIVERSITY COLLEGE CARDIFF CONSULTANTS LTD. If there are other authors, they declare that they have no known competing financial interests or personal relationships that could have appeared to influence the work reported in this paper.

Data availability

Data will be made available on request.

Acknowledgements

F.P acknowledge support from the Life Science Research Network Wales.

G.R., F.C., A.F. acknowledge support from the Project CH4.0 under the MUR program "Dipartimenti di Eccellenza 2023–2027" (CUP: D13C22003520001).

Dr. Lloyd Evans (Cardiff School of Bioscience) is acknowledged for his fruitful insights and discussion about potential applications of Fingolimod prodrugs in Niemann-Pick and MLIV lysosomal storage diseases.

Supplementary materials

Supplementary material associated with this article can be found, in the online version, at doi:10.1016/j.molstruc.2024.138614.

References

[1] K. Thomas, T. Sehr, U. Proschmann, F.A. Rodriguez-Leal, R. Haase, T. Ziemssen, J. Neuroinflamm. 14 (2017) 41.
[2] A. Billich, F. Bornancin, P. Dévay, D. Mechtcheriakova, N. Urtz, T. Baumruker, J. Biol. Chem. 278 (2003) 47408–47415.
[3] S.W. Paugh, S.G. Payne, S.E. Barbour, S. Milstien, S. Spiegel, FEBS Lett. 554 (2003) 189–193.
[4] L.D. Weinstock, A.M. Furness, S.S. Herron, S.S. Smith, S.B. Sankar, S.G. DeRosa, D. Gao, M.E. Mepyans, A. Scotto Rosato, D.L. Medina, A. Vardi, N.S. Ferreira, S. M. Cho, A.H. Futerman, S.A. Slaugenhaupt, L.B. Wood, Y. Grishchuk, Hum. Mol. Genet. 27 (2018) 2725–2738.
[5] N.C. Hait, L.E. Wise, J.C. Allegood, M. O'Brien, D. Avni, T.M. Reeves, P.E. Knapp, J. Lu, C. Luo, M.F. Miles, S. Milstien, A.H. Lichtman, S. Spiegel, Nat. Neurosci. 17 (2014) 971–980.
[6] N.H. Pipalia, C.C. Cosner, A. Huang, A. Chatterjee, P. Bourbon, N. Farley, P. Helquist, O. Wiest, F.R. Maxfield, Proc. Natl. Acad. Sci. U.S.A. 108 (2011) 5620–5625.
[7] D. Lombardo, M.A. Kiselev, S. Magazù, P. Calandra, Adv. Cond. Matt. Phys. 2015 (2015) 151683.
[8] a) G. Gasparini, E.-K. Bang, J. Montenegro, S. Matile, Chem. Commun. 51 (2015) 10389–10402;
b) S. Matile, A. Vargas Jentzsch, J. Montenegro, A. Fin, Chem. Soc. Rev. 40 (2011) 2453–2474.
[9] a) C. Morozzi, J. Sedlakova, M. Serpi, M. Avigliano, R. Carbajo, L. Sandoval, Y. Valles-Ayoub, P. Crutcher, S. Thomas, F. Pertusati, J. Med. Chem. 62 (2019) 8178–8193;
b) M. Serpi, F. Pertusati, Expert. Opin. Drug Discov. 16 (2021) 1149–1161;
c) M.A. Vanden Avond, H. Meng, M.J. Beatka, D.C. Helbling, M.J. Prom, J. L. Sutton, R.A. Slick, D.P. Dimmock, F. Pertusati, M. Serpi, E. Pileggi, P. Crutcher, S. Thomas, M.W. Lawlor, J. Inherit. Metab. Dis. 44 (2021) 492–501;
d) M. Serpi, R. Bibbo, S. Rat, H. Roberts, C. Hughes, B. Caterson, M.J. Alcaraz, A. T. Gibert, C.R. Verson, C. McGuigan, J. Med. Chem. 55 (2012) 4629–4639.
[10] E. James, F. Pertusati, A. Brancale, C. McGuigan, Bioorg. Med. Chem. Lett. 27 (2017) 1371–1378.
[11] M. Serpi, K. Madela, F. Pertusati, M. Slusarczyk, Curr. Protoc. Nucl. Acid Chem. 53 (2013), 15.15.11–15.15.15.
[12] F. Pertusati, S. Serafini, N. Albadry, R. Snoeck, G. Andrei, Antivir. Res. 143 (2017) 262–268.
[13] E. Lloyd-Evans, F. Pertusati, J. Edwards, E. Maguire, C. McGuigan, (Ed.: U. C. C. C. Ltd), 2018.
[14] M. Serpi, K. Madela, F. Pertusati, M. Slusarczyk, Curr. Protoc. Nucl. Acid Chem (2013). Chapter 15, Unit15 15.
[15] a) R.W. Sinkeldam, N.J. Greco, Y. Tor, Chem. Rev. 110 (2010) 2579–2619;
b) C. Bellomo, D. Zanetti, F. Cardano, S. Sinha, M. Chaari, A. Fin, A. Maranzana, R. Núñez, M. Blangetti, C. Prandi, Dyes Pigm. 194 (2021) 109644.
[16] a) G. Renno, F. Cardano, G. Volpi, C. Barolo, G. Viscardi, A. Fin, Molecules 27 (2022) 3856;
b) G. Renno, F. Cardano, V. Ilieva, G. Viscardi, A. Fin, Eur. J. Org. Chem. (2022);
c) D.A. Doval, A. Fin, M. Takahashi-Umebayashi, H. Riezman, A. Roux, N. Sakai, S. Matile, Org. Biol. Chem. 10 (2012) 6087–6093.
[17] S. Fery-Forgues, J.-P. Fayet, A. Lopez, J. Photochem. Photobiol., A 70 (1993) 229–243.
[18] Q. Meng, Y. Shi, C. Wang, H. Jia, X. Gao, R. Zhang, Y. Wang, Z. Zhang, Org. Biol. Chem. 13 (2015) 2918–2926.
[19] L.D. Lavis, R.T. Raines, ACS Chem. Biol. 3 (2008) 142–155.
[20] C. Jiang, H. Huang, X. Kang, L. Yang, Z. Xi, H. Sun, M.D. Pluth, L. Yi, Chem. Soc. Rev. 50 (2021) 7436–7495.
[21] A. Brouwer, M., *Pure Appl. Chem.* 83 (2011) 2213–2218.
[22] a) B. Schininà, A. Martorana, N.A. Colabufo, M. Contino, M. Niso, M.G. Perrone, G. De Guidi, A. Catalfo, G. Rappazzo, E. Zuccarello, O. Prezzavento, E. Amata, A. Rescifina, A. Marrazzo, RSC Adv. 5 (2015) 47108–47116;
b) M. Onoda, S. Uchiyama, T. Santa, K. Imai, Luminescence 17 (2002) 11–14.

[23] R. Brahma, H. Raghuraman, J. Membr. Biol. 255 (2022) 469–483.
[24] C. Angeletti, J. Wylie Nichols, Biochemistry 37 (1998) 15114–15119.
[25] a) C.-J. Weng, J.-P. Wu, M.-Y. Kuo, Y.-W. Hsueh, Mol. Membr. Biol. 33 (2016) 23–28;
b) A. Lajevardipour, J.W.M. Chon, A. Chattopadhyay, A.H.A. Clayton, Sci Rep 6 (2016) 37038;
c) G. Li, J. Kim, Z. Huang, J.R.S. Clair, D.A. Brown, E. London, Proc. Natl. Acad. Sci. U.S.A. 113 (2016) 14025–14030.
[26] A. Chattopadhyay, Chem. Phys. Lipids 53 (1990) 1–15.
[27] a) F.S. Abrams, E. London, Biochem 32 (1993) 10826–10831;
b) D. Huster, P. Müller, K. Arnold, A. Herrmann, Biophys. J. 80 (2001) 822–831.
[28] P. Buehlmayer, K. Hinterding, C. Spanka, F. Zecri, NOVARTIS AG [CH]/[CH] (2004), 25.03.
[29] D.W. Brown, M.F. Mahon, A. Ninan, M. Sainsbury, J. Chem. Soc. Perkin Trans. 1 (1997) 2329–2336.
[30] Z. Huang, R.P. Haugland, Biochem. Biophys. Res. Commun. 181 (1991) 166–171.